Stanford Exploration Project, Report 97, July 8, 1998, pages 95–116

The azimuth moveout operator for vertically inhomogeneous media

Tariq Alkhalifah and Biondo L. Biondi[1]

keywords: *AMO, DMO, dip moveout*

ABSTRACT

The azimuth moveout (AMO) operator, unlike the DMO operator, has a 3-D structure in homogeneous isotropic media, with an out-of-plane (crossline) component. In general, this component is concaved downward giving the operator an overall skewed-saddle shape. The AMO operator is typically smaller in size than conventional DMO operators. When velocity varies vertically, the operator shape changes depending on how the velocity varies. The general shape of the operator, however, remains overall saddle. In fact, for smooth velocity increases with depth, similar to those found in the Gulf of Mexico, the AMO operator does not vary much from its homogeneous counterpart. The residual AMO operator, constructed by cascading a forward homogeneous AMO operator with an inverse $v(z)$ one is extremely small, which suggests that the impact of such $v(z)$ variations on the AMO operator is generally small. Complex vertical velocity variations, on the other hand, result in more complicated AMO operators that include, among other things, triplications at moderate angles. Regardless of the complexity of the model, the $v(z)$ operator has the same first order behavior as its homogeneous counterpart. As a result, for small dip angles the homogeneous AMO, as a tool for partial stacking, often enhances the image. Moderate to steep dips in complex $v(z)$ media requires the application of an algorithm that honors such velocity variations.

INTRODUCTION

For cost reasons, seismic surveys are designed so that multiple geophone arrays are deployed to record sound waves, typically emanating from a single source. These geophones, in a 3-D survey, are rarely aligned along a single straight line that passes through the source. This is the case in most 3-D marine, as well as land, survey designs. As a result, the source-receiver azimuth is not constant and in typical marine data, can range between -45 to 45 degrees, where 0 azimuth is the direction of the ship motion (Biondi et al., 1998). Most prestack imaging algorithms (i.e., dip moveout

[1]**email:** tariq@sep.stanford.edu,biondo@sep.stanford.edu

and prestack migration) are theoretically designed to work with data acquired along a single source-receiver azimuth. Azimuth variation is often ignored and seismic traces are binned, after normal-moveout (NMO) correction, into a regularly sampled data set in offset and Common midpoint (CMP). Though, for isotropic homogeneous media, such binning has no bearing on reflections from horizontal events, ignoring the azimuth variation can harm reflections from dipping events (Biondi et al., 1998), resulting in the attenuation of such reflections when partial stacking is applied to reduce the volume of the data set (Hanson and Witney, 1995).

Biondi et al. (1998) introduced azimuth moveout correction (AMO) as a single operator to correct for azimuth variations in homogeneous isotropic media. They analytically derived the AMO operator, and used it in a Kirchhoff-type of implementation on multi-azimuth seismic data sets. Though the AMO operator had a 3-D structure, it had an overall small aperture, thus the Kirchhoff implementation of AMO is relatively cheap. Figure 1 shows an AMO operator in homogeneous media. It is clearly 3-D in structure and has a general skewed saddle shape. Like the DMO

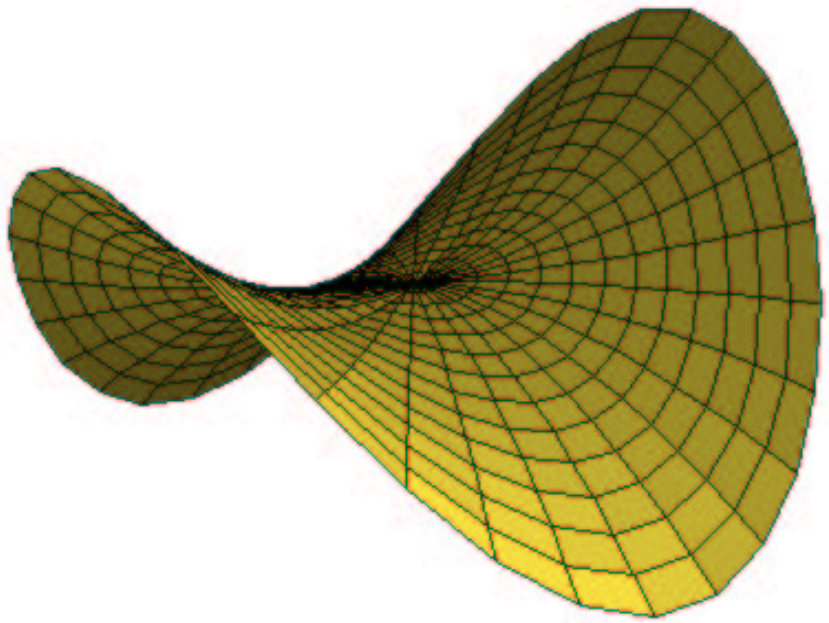

Figure 1: An AMO operator for a homogeneous medium with velocity equal to 2 km/s. The offset is 2 km and the input normal-moveout (NMO) corrected time is 2 s. tariq1-amo-homo30r [NR]

operator, the AMO operator is applied after NMO correction. Despite the simplicity of the homogeneous-medium AMO operator and its application, the earth subsurface is rarely homogeneous. Velocity increase with depth is very common in the subsurface, and an important question is how much of an error can be attributed to ignoring such vertical velocity variation. Using the 3-D SEG/EAEG salt-dome model, Biondi

(1998) shows that the homogeneous AMO operator produces reasonable results in smooth vertical velocity variations. Is this a general conclusion or only holds for the cases he tested?

Through the combined action of gravity and sedimentation, velocity variation with depth represents the most important first-order inhomogeneity in the Earth subsurface. This is one reason why time migration works well in so many places. Therefore, studying the AMO operator for such 1-D models can be useful in many parts of the Earth, and since the AMO operator is generally small, the $v(z)$ AMO operator might be useful even in relatively complex areas.

In this paper, we will numerically construct the AMO operator for vertically inhomogeneous media, as well as observe how the operator shape is influenced by vertical inhomogeneity. Next, we will generate the residual AMO operator constructed by cascading a forward homogeneous-medium AMO operator and an inverse $v(z)$-medium AMO operator. The size and shape of the residual operator provides us with valuable information regarding the impact of vertical inhomogeneity on AMO. The smaller the residual operator the lesser the impact of vertical velocity gradients on AMO. Examples will include three types of vertical velocity variations: linear increase as a function of depth, a low velocity layer embedded in an overall increase in velocity with depth, and a high velocity layer embedded in an increase in velocity with depth. The last example is similar to what can be observed in the North Sea, as a result of the Austin Chalk layer.

AZIMUTH MOVEOUT CORRECTION IN HOMOGENEOUS MEDIA

The impulse response of the AMO operator in homegeneous media is a skewed saddle. The shape of the saddle depends on the offset vector of the input data $\mathbf{h}_1 = h_1 \cos\theta_1 \mathbf{x} + h_1 \sin\theta_1 \mathbf{y} = h_1(\cos\theta_1, \sin\theta_1)$ and on the offset vector of the desired output data $\mathbf{h}_2 = h_2(\cos\theta_2, \sin\theta_2)$, where the unit vectors $\mathbf{x}$ and $\mathbf{y}$ point respectively in the in-line direction and the cross-line direction. The time shift to be applied to the data is a function of the difference vector $\mathbf{\Delta m} = \Delta m(\cos\Delta\varphi, \sin\Delta\varphi)$ between the midpoint of the input trace and the midpoint of the output trace. The analytical expression of the AMO saddle, is

$$t_2\left(\mathbf{\Delta m}, \mathbf{h}_1, \mathbf{h}_2, t_1\right) = t_1 \frac{h_2}{h_1} \sqrt{\frac{h_1^2 \sin^2(\theta_1 - \theta_2) - \Delta m^2 \sin^2(\theta_2 - \Delta\varphi)}{h_2^2 \sin^2(\theta_1 - \theta_2) - \Delta m^2 \sin^2(\theta_1 - \Delta\varphi)}}. \tag{1}$$

The traveltimes t_1 and t_2 are respectively the traveltime of the input data after NMO has been applied, and the traveltime of the results before inverse NMO has been applied.

Figure 2 shows three AMO operators that correspond to three different azimuth correction angles in a homogeneous medium. From left to right, the azimuth corrections are 15, 30, and 45 degrees, respectively. The input and output offset were

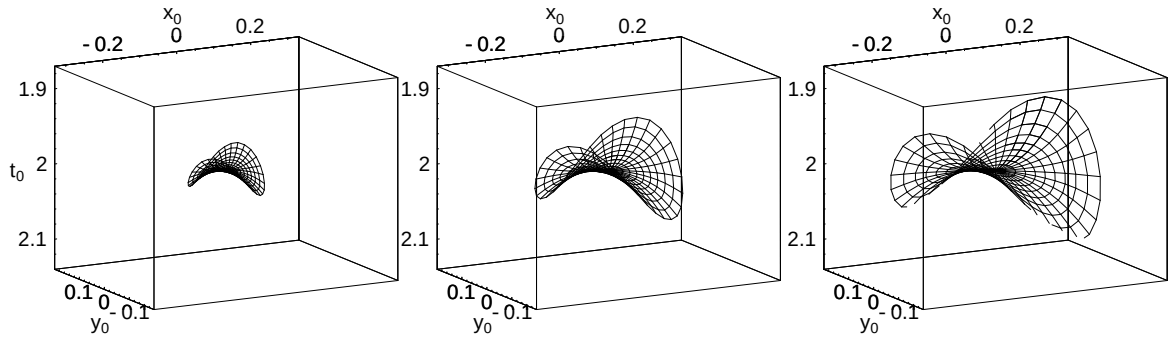

Figure 2: AMO operators for isotropic homogeneous media for an input and output offset of 2 km and correction to only the azimuth. The azimuth corrections from left plot to right are 15, 30, and 45 degrees, respectively. The velocity of the homogeneous isotropic medium is 2 km/s, and the input NMO corrected time is 2 s. The x_0 (inline) and y_0 (crossline) axis are in km and the t_0 is in seconds. This holds here and throughout. The circular lines are contours of equal ray parameter. tariq1-Amo-homo3 [NR]

the same and equal to 2 km. Though the general shape of the AMO operator is practically the same between the three operators, the size is very much dependent on the amount of azimuth correction; the larger the azimuth correction the larger the AMO operator. Clearly, for zero azimuth correction the operator reduces to a point. The size dependence of the operator on azimuth holds regardless of the medium. The shape of the operator, however, is very much independent of azimuth correction.

In Figure 2 and throughout, the contour curves plotted represent lines of equal ray parameter. It provides information on the distribution of dip angles, as well as on the distribution of energy along the operator; denser contour lines imply higher amplitude.

GENERATING THE AZIMUTH MOVEOUT OPERATOR IN V(Z) MEDIA

We build the AMO operator in $v(z)$ media by cascading a forward and an inverse 3-D $v(z)$ DMO operators. An angular transformation, that depends on the azimuth correction, is applied to the inverse operator. Therefore, to build the AMO operator we must first build the 3-D $v(z)$ operator. Artley et al. (1993) suggested an approach to build a kinematically exact 3-D DMO operator. Following their approach, we construct the 3-D DMO operator by solving a system of six nonlinear equations to obtain six unknowns that include, among other things, the zero-offset time and surface position of the specular reflection point. Artley's traveltimes are calculated and tabulated using an isotropic $v(z)$ ray tracing. Because velocity varies only vertically, each ray propagating in the subsurface is contained in a vertical plane; therefore, 2-D

raytracing is sufficient to calculate the traveltimes. The total traveltime is:

$$t_{sg} = t_s + t_g,$$

and therefore the gradient vector,

$$\bigtriangledown t_{sg} = \bigtriangledown t_s + \bigtriangledown t_g = \mathbf{p_s} + \mathbf{p_g}$$

has a direction that is normal to reflector dip. Because the zero-offset slowness vector $\mathbf{p_0}$ is also in the direction that is normal to reflector dip, then $\mathbf{p_0}$ is a scaled sum of the slownesses of the rays from the source $\mathbf{p_s}$ and receiver $\mathbf{p_g}$ to the specular point reflection. Therefore,

$$\mathbf{p_0} = \lambda(\mathbf{p_s} + \mathbf{p_g}). \tag{2}$$

Considering the z-component gives

$$p_{0z} = \lambda(p_{sz} + p_{gz}),$$

then

$$\lambda = \frac{p_{0z}}{p_{sz} + p_{gz}}.$$

Since

$$p_{0z} = \cos[\theta(p_0, t_0)]s(t_0),$$

$$p_{sz} = \cos[\theta(p_s, t_s)]s(t_s),$$

and

$$p_{gz} = \cos[\theta(p_g, t_g)]s(t_g),$$

where s (=$|\mathbf{p}|$; for each of $\mathbf{p_s}$, $\mathbf{p_g}$, and $\mathbf{p_0}$) is the slowness and θ is the ray angle. Then

$$\lambda = \frac{\cos[\theta(p_0, t_0)]s(t_0)}{\cos[\theta(p_s, t_s)]s(t_s) + \cos[\theta(p_s, t_s)s(t_s)}. \tag{3}$$

Substituting equation (3) into the x-and y-components of equation (2) provides two of the six nonlinear equations needed to be solved. The other four equations are:

$$0 = \xi(p_g, t_g)\cos\phi_g - \xi(p_s, t_s)\cos\phi_s + 2h \tag{4}$$

$$0 = \xi(p_g, t_g)\sin\phi_g - \xi(p_s, t_s)\sin\phi_s \tag{5}$$

$$0 = \tau(p_0, t_0) - \tau(p_s, t_s) \tag{6}$$

$$0 = \tau(p_0, t_0) - \tau(p_g, t_g). \tag{7}$$

Equation (4) is the requirement that the surface distances, ξ, along the inline component from both the source and receiver to the specular reflection point (SRP) add to equal the source-receiver offset, $2h$. Equation (5) is the requirement that the distances along the crossline component to the SRP are equal for the source and receiver. Equations (6) and (7) imply that the vertical times, τ from the source, the receiver,

and the zero-offset surface positions to the SRP are equal. Both ξ and τ are calculated using ray tracing and then stored in a table as a function of ray parameter p and the traveltime t.

The inverse operator is calculated in the same way as the forward operator, but now we must calculate t_n or the total traveltime t_{sg} instead of t_0, which is known. Subsequently, x_0 and y_0 are calculated in the same way as the forward approach.

To build the AMO operator, the output of the forward 3-DMO operator $t_0(t_n, p_x, p_y)$, $x_0(t_n, p_x, p_y)$, and $y_0(t_n, p_x, p_y)$ are inserted into the inverse 3-D DMO operator. Prior to applying the inverse operator the axes are rotated with an angle given by the desired azimuth correction. The result is an AMO operator given by

$$t_{AMO}[t_0(t_n, p_x, p_y), p_x, p_y],$$

$$x_{AMO}(t_n, p_x, p_y) = x_0(t_n, p_x, p_y) - x_0^{'}(t_0, p_x, p_y),$$

and

$$y_{AMO}(t_n, p_x, p_y) = y_0(t_n, p_x, p_y) - y_0^{'}(t_0, p_x, p_y),$$

where $x_0^{'}$ and $y_0^{'}$ correspond to the adjoint (inverse) operator in the rotated domain. The rotation angle is the azimuth correction angle.

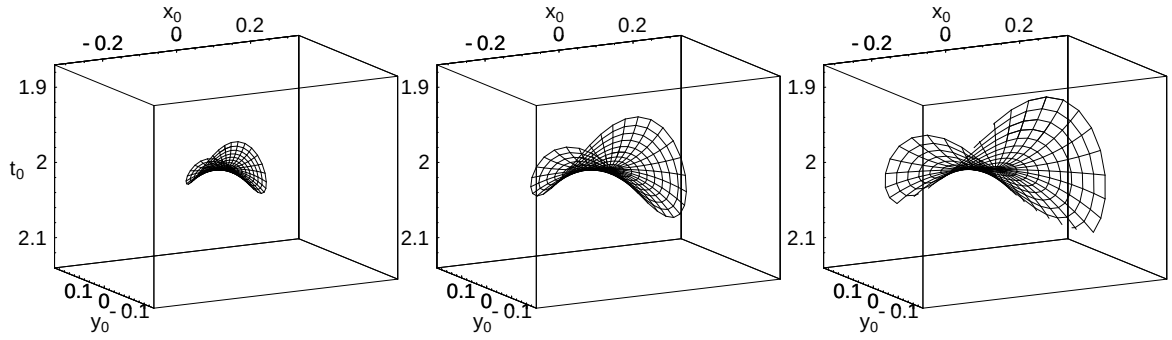

Figure 3: AMO operators for $v(z)$ media for an input and output offset of 2 km and correction to only the azimuth. The azimuth corrections from left plot to right are 15, 30, and 45 degrees, respectively. The velocity varies with depth linearly as $v(z) = 1.5 + 0.6z$ km/s, and the input NMO corrected time is 2 s. tariq1-Amo-vz3 [NR]

Figure 3 shows three AMO operators that correspond to three different azimuth correction angles in a $v(z)$ medium. From left to right, the azimuth correction angles are 15, 30, and 45 degrees, respectively. The input and output offset are the same and equal to 2 km. The root-mean-square (rms) velocity for this model is similar to the homogeneous one and is equal to 2 km/s. Interestingly, these operators are very similar to the respective homogeneous ones. The subtle differences, however, will be apparent when we generate the residual AMO operators. Though the shape of the AMO operator is practically the same between the three corrections, the size is very

much dependent on the amount of azimuth correction; the larger the azimuth angular correction the larger the AMO operator. This phenomenon occurs for homogeneous as well as $v(z)$ media. As a result, we will use a single azimuth correction for most of the examples shown in this paper, that is a 30 degrees azimuth correction. Figure 4

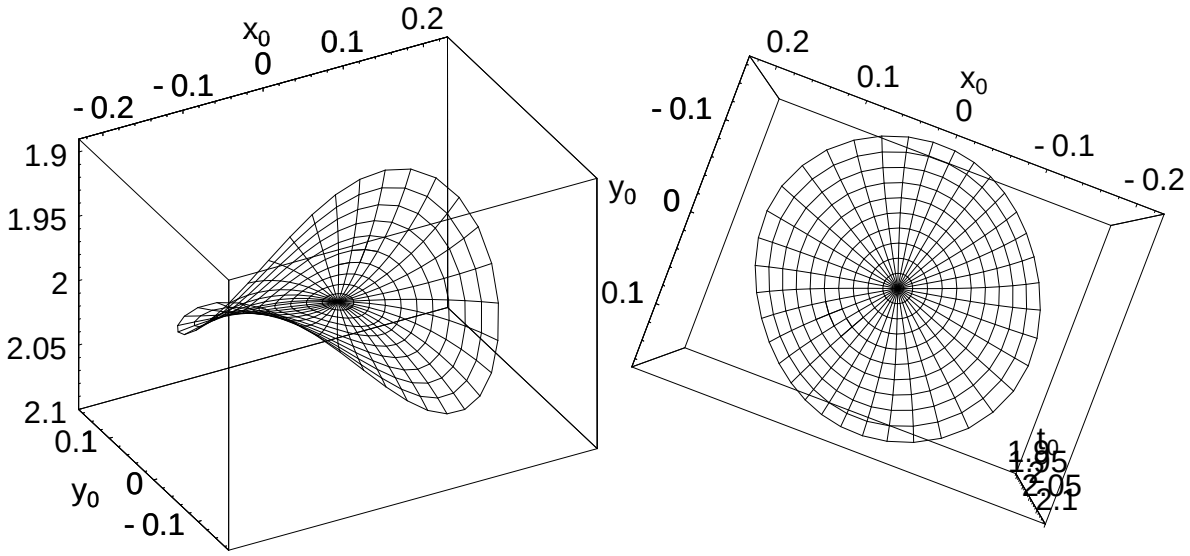

Figure 4: An upper side (left) and a top (right) view of the AMO operator for a linear $v(z)$ medium for an input and output offset of 2 km and correction to only the azimuth of 30 degrees. tariq1-Op2vzlin [NR]

shows an upper side and a top view of the 30-degrees correction AMO operator for the $v(z)$ medium. The saddle is altered 30 degrees from the inline direction, in agreement with the amount of azimuth correction applied. The AMO operator domain has an overall circular shape. The shape of our AMO domain appears to be different from the one presented by Biondi et al. (1998) (a parallelogram), because we limit the zero-offset ray parameters when plotting the AMO operator.

AMO OPERATORS IN $V(Z)$ MEDIA

Three examples of vertical velocity variations with depth are considered here. All three examples are plausible, and can be found in the subsurface, however, they do not represent all possible vertical velocity variations in the subsurface. These examples will, however, provide us with a reasonable understanding on how the AMO operator is sensitive to vertical inhomogeneity. We will show three different AMO operators; the first corresponding to a correction in offset only, called typically the residual DMO operator. The second corresponding to a correction in offset and azimuth, with an azimuth correction of 30 degrees. The third has no offset correction, but an azimuth correction of 30 degrees. The offset correction, used in most of the examples, is from

2.0 km to 1.5 km. For size comparison, we, also, display the full $v(z)$ DMO operator for an offset of 2 km. The NMO time for all operators in this paper is 2 s.

All the 3-D graphs of AMO operators include an aperture that covers half the maximum possible zero-offset ray parameter. Since the surface velocity for all three models is the same at 1.5 km/s, this range includes ray emergence angle up to 30 degrees. The corresponding reflector dip angle, however, should be much higher since velocity increases with depth, and it will depend on the velocity model. The 2-D operator cross-sections, on the other hand, will include emerging angles up to the critical angle. Figure 5 shows two of the three velocity models considered in this paper. The left one will be referred to as the low-velocity-layer example, while the right one will be referred to as the high-velocity-layer example. The third velocity model, not shown here, is a simple linear velocity increase with depth at a gradient of $0.6s^{-1}$. All velocity models have a surface velocity of 1.5 km/s.

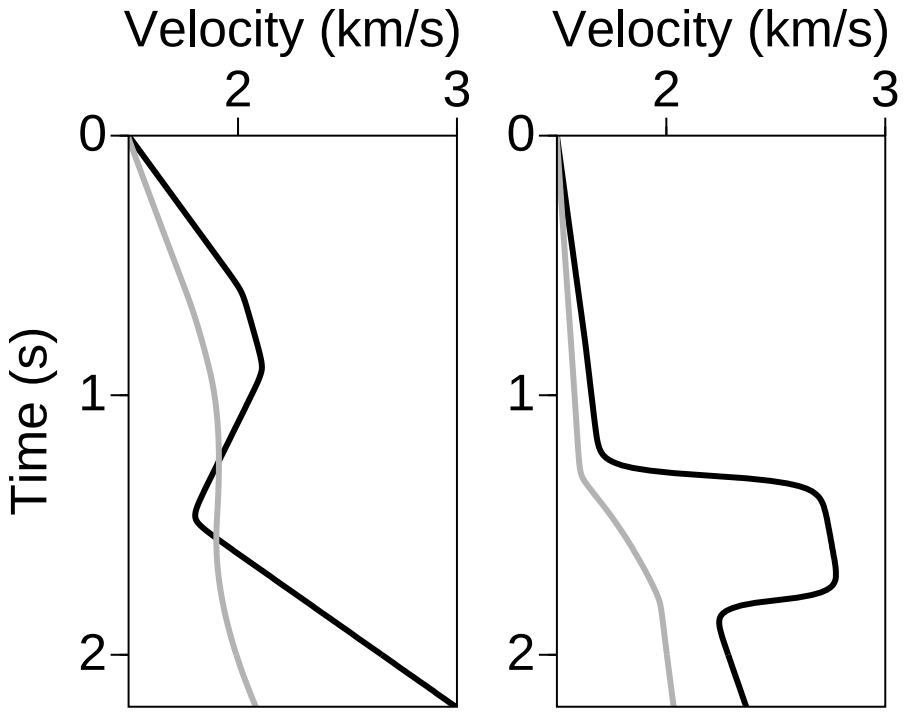

Figure 5: Velocity models given a function of vertical time. The black curves are the interval velocities, while the gray curves are rms velocities. All the models considered in this paper have an rms velocity of about 2 km/s at 2 s vertical time. tariq1-vel [NR]

Figure 6 shows the AMO operators for the first example, which is a linear velocity increase will depth. The AMO operator corresponding to a pure offset correction,

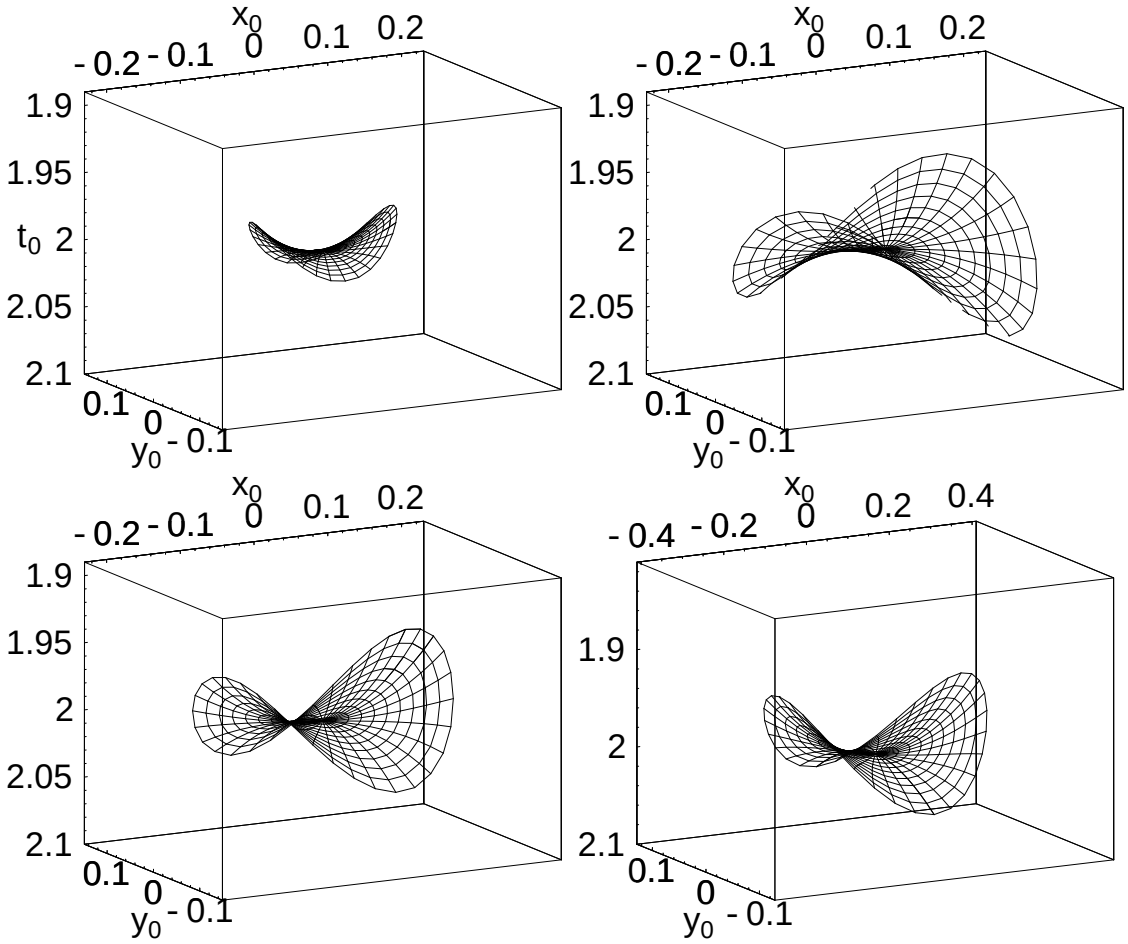

Figure 6: Four AMO operators in the linear $v(z)$ model. The upper left operator corresponds to a correction in offset only, or residual DMO, the upper right operator corresponds to a correction in azimuth only, the lower left corresponds to a correction in both offset and azimuth, while the lower right operator is the 3-D $v(z)$ DMO operator. The full 3-D DMO operator is drawn at a large scale, and as a result, appears to be smaller than the rest of the operators. tariq1-Op4vzlin2 [NR]

shown upper left, has a similar shape to the full 3-D DMO operator, shown lower-right, which is generally a saddle, but much smaller in size. The corresponding residual DMO operator for homogeneous media is a purely 2-D operator. The azimuth-correction-only operator, shown upper right, is very similar to the homogeneous-medium one shown in Figure 2, with an overall skewed saddle shape. When the offset and azimuth corrections are combined in a single operator, it is given by the one shown in the lower left of Figure 6. The full DMO operator, shown in the lower-right, is clearly the largest in size. AMO operators that include offset correction alters the

position of horizontal, as well as dipping reflections. This alteration is necessary to correct for the non-hyperbolic moveout associated with $v(z)$ media for horizontal and dipping events.

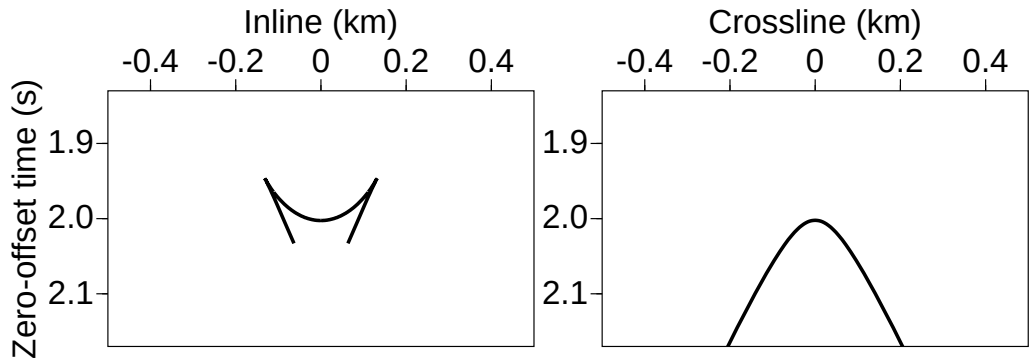

Figure 7: The inline and crossline components of the AMO operator (or residual DMO) shown in Figure 6 (upper-left), but with a wider aperture which includes the triplication. This operator, as previously stated, applies an offset correction from 2.0 km to 1.5 km. tariq1-incrossvzlin2 [NR]

Figure 7 shows the inline and crossline components of the AMO operator shown in Figure 6 (upper-left), which corrects for offset only from 2 km to 1.5 km. The operator here includes the full aperture of the AMO operator, and thus includes the triplication at high angles. Surprisingly, the size of the operator in the crossline component is larger than that in the inline component. This fact stresses the importance of the crossline component of the residual DMO operator. Figure 8 shows the inline and crossline components of the AMO operator corresponding to azimuth correction of 30 degrees. Again, we include the full possible aperture and conveniently no triplications exist. The absence of triplications simplify the application of such an operator in a Kirchhoff type of implementation. Figure 9 shows the inline and crossline components of the AMO operator that includes both the offset and azimuth corrections. This operator includes triplications that are associated with the offset correction portion of the operator. This operator is simply the convolution of the two previous operators, with its overall shape resembling both operators.

An AMO (or residual DMO) correction from offset 1.5 to 2.0 km will provide us with an operator that is inverse (or adjoint) to the operator shown in Figure 7, which corresponds to an offset correction from 2.0 to 1.5 km. Figure 10 shows the inline and crossline components of such an AMO operator with the full aperture included. Triplications similar but opposite to the ones shown in Figure 7 appear here. The convolution of the operators in Figure 7 and Figure 10 should result in an impulse, which confirms the dot-product rule.

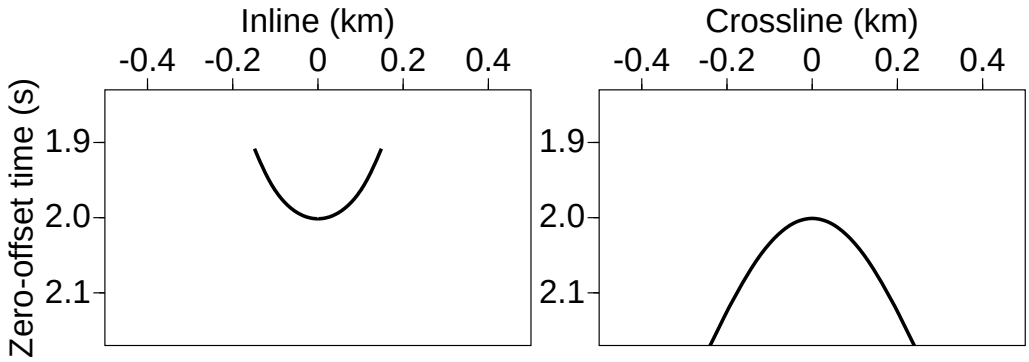

Figure 8: The crossline and inline components of the AMO operator shown in Figure 6 (upper-right), but with a wider aperture. This operator, as previously stated, applies only an azimuth correction of 30 degrees and clearly does not include triplications. tariq1-incrossvz30onlin2 [NR]

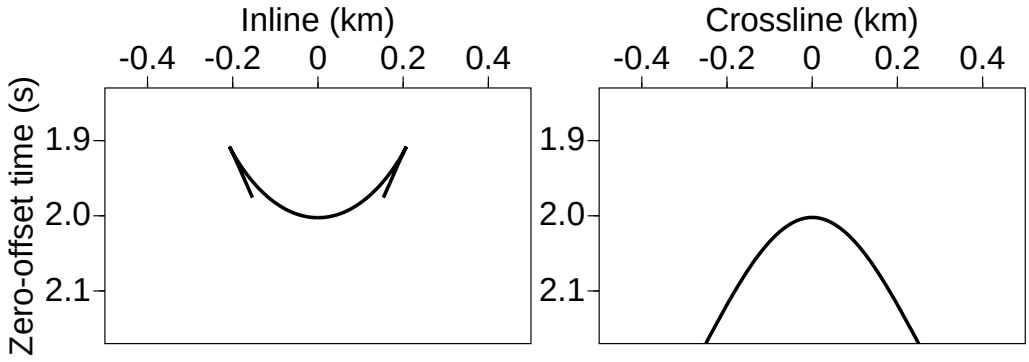

Figure 9: The crossline and inline components of the AMO operator shown in Figure 6 (lower-left), but with a wider aperture which includes the triplication. This operator, as previously stated, applies an azimuth correction of 30 degrees, as well as, offset correction from 2.0 km to 1.5 km. tariq1-incrossvz30lin2 [NR]

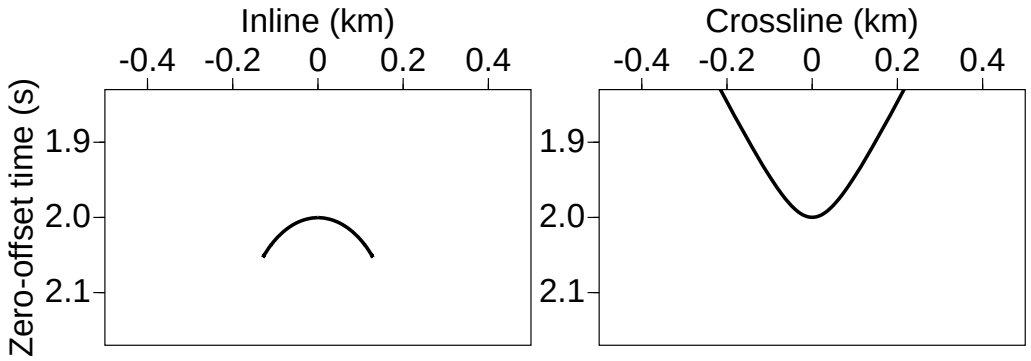

Figure 10: The crossline and inline components of the AMO operator (or residual DMO) that is the inverse (or adjoint) of that shown in Figure 7. This operator applies an offset correction from 1.5 km to 2 km. tariq1-incrossvzlin [NR]

The second example has a low velocity zone as shown in Figure 5 (left). Figure 11 shows AMO operators for such a velocity model: corresponding to a pure offset correction (upper left), corresponding to a pure azimuth correction (upper right), corresponding to the combination of offset and azimuth correction (lower left), and corresponding to a full DMO operator (plotted at a larger scale, lower right). The operators that include offset corrections are much more complicated then the ones corresponding to the linear velocity model example, while the operator that includes only azimuth corrections are very similar to the linear velocity model ones, as well as to the homogeneous model ones. This observation implies that vertical inhomogeneity has a greater impact on the offset correction part of the operator than the azimuth correction part.

A closer look given by the inline and crossline components shown in Figure 12 reveals the complications added to the operator by the offset correction. Specifically, the crossline component includes triplications at low reflector angles. These triplications will make any Kirchhoff-type application of this operator difficult. The AMO operator corresponding to only azimuth correction, on the other hand, does not include triplications at any angle, as shown in Figure 13. The absence of triplications, despite the presence of a low velocity zone, is encouraging.

Figure 14, also, shows the four AMO operators, however, now for the complicated high-velocity layer model. Again the AMO operators are smaller in general than the full DMO operator shown at lower right. Interestingly, the full DMO operator and the residual DMO operator (upper left) have small crossline components, and in this aspect, they are similar to the constant-velocity operator. The azimuth correction gives the AMO operator a more 3-D shape as shown in Figure 14 (upper-right and lower-left). Again, the AMO operator that includes only azimuth correction (of 30

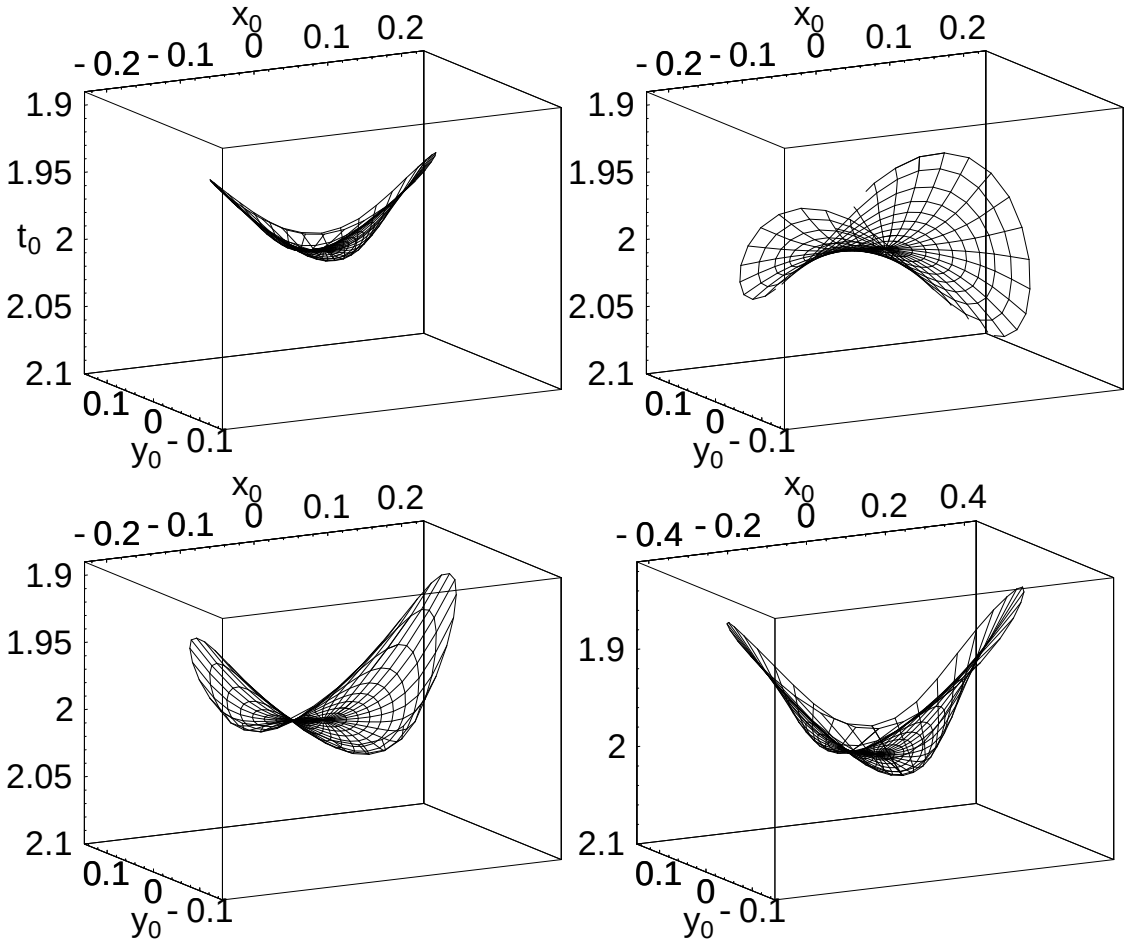

Figure 11: Same as in Figure 6 but using the low-velocity-layer model shown in Figure 5 (left). tariq1-Op4vzlow [NR]

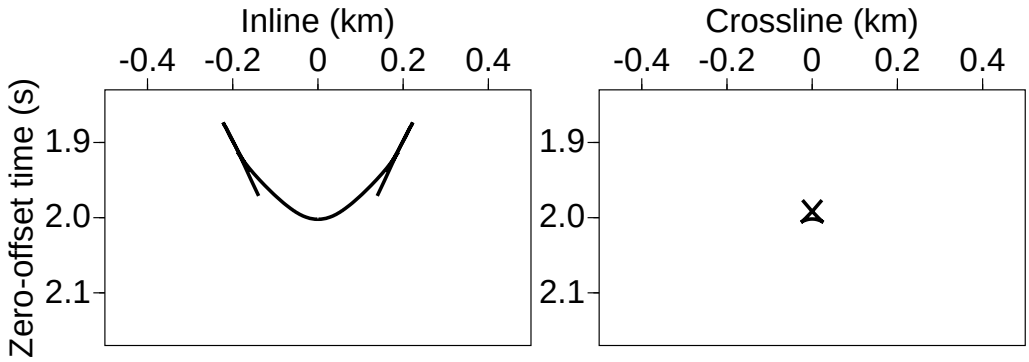

Figure 12: The crossline and inline components of the AMO operator (or residual DMO) shown in Figure 11 (upper-left), but with a wider aperture which includes all triplications. This operator applies an offset correction from 2.0 km to 1.5 km. tariq1-incrossvzlow [NR]

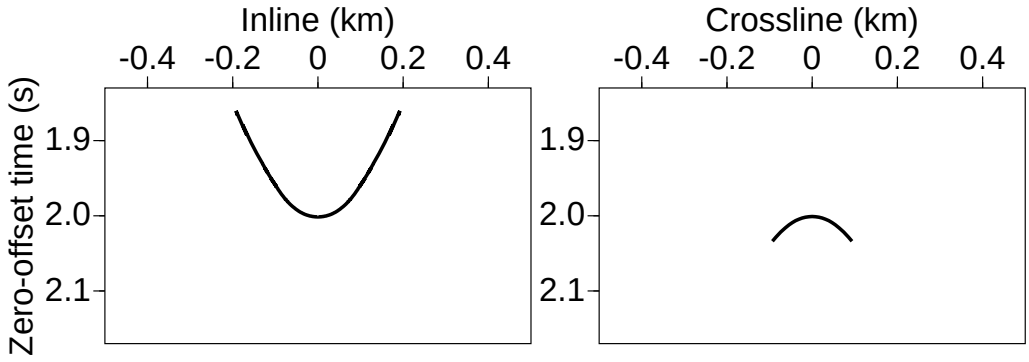

Figure 13: The crossline and inline components of the AMO operator shown in Figure 11 (upper-right), but with a wider aperture. This operator, as previously stated, applies only an azimuth correction of 30 degrees and clearly does not include triplications. tariq1-incrossvz30onlow [NR]

degrees) does not include triplication.

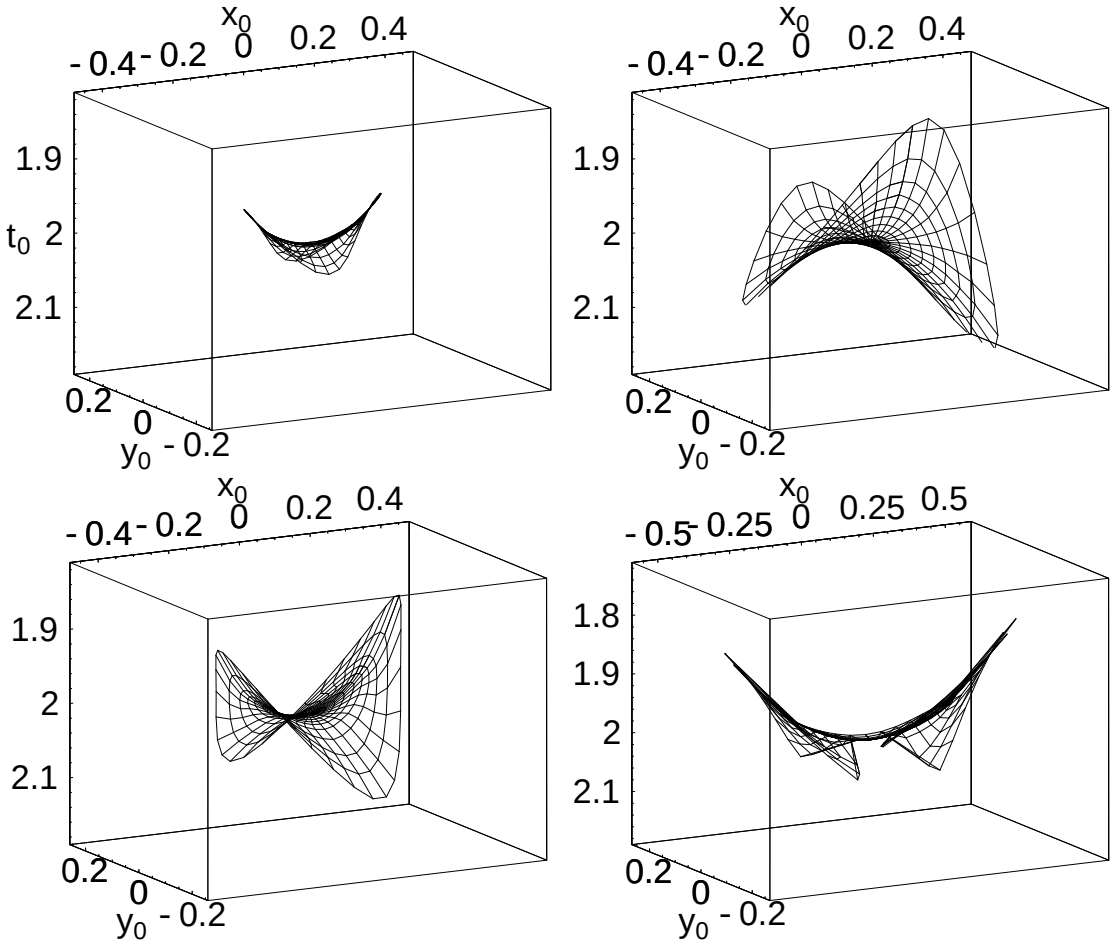

Figure 14: Same as in Figure 6 but using the high-velocity-layer model shown in Figure 5 (right). tariq1-Op4vzhigh [NR]

In summary, AMO operators correcting only the azimuth are much simpler than those that correct also the offset. These azimuth-only correction operators are overall triplication free, even for the case of the high velocity layer. Therefore, using such operators in Kirchhoff-type implementation should be straightforward. These operators are also, for the smooth velocity examples, very similar to the constant-velocity AMO operators.

THE RESIDUAL AMO OPERATOR

The residual AMO operator includes a cascade of four 3-D $v(z)$ DMO operations; two forward operations and two inverse ones. The difference between each of the pair of forward and inverse operations is the medium parameters. For example, a pair of

forward and inverse DMO's, or AMO, is applied for a homogeneous medium followed by another pair corresponding to a $v(z)$ medium. The result is a residual AMO operator that corrects for the velocity perturbation from a background homogeneous model to a $v(z)$ one.

The size of the residual AMO operator is directly dependent on the amount of velocity perturbation from the homogeneous background model. The residual operator provides information on the impact of the perturbation in velocity on the AMO operator. The smaller the size of the residual operator, the lesser the velocity variations influenced the AMO operator, and thus the lesser the need to use it.

Figure 15 shows a side and a top view of a residual AMO operator that corrects a homogeneous AMO operator to a linear-velocity AMO operator. In other words, this residual AMO operator, when convolved with the homogeneous-medium AMO operator, provides us with the linear-velocity AMO operator. This AMO operator corresponds to a pure azimuth correction of 30 degrees. The resulting residual operator is about 10 times smaller than the corresponding full AMO operator shown in Figure 6 (upper-right). In fact, the maximum time correction exerted by this residual AMO operator is less than 10 ms, even for dips around 50 degrees. Such corrections are very much insignificant, and the homogeneous medium AMO operator is sufficient to correct for azimuth in such $v(z)$ velocity variations.

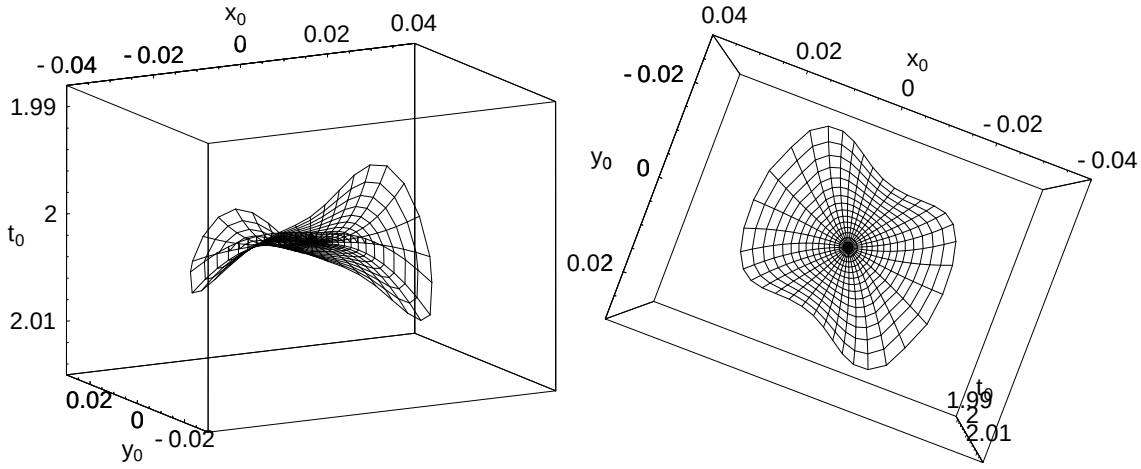

Figure 15: A side (left) and a top (right) view of a residual AMO operator responsible for the correction from the linear velocity model to a homogeneous medium for a pure azimuth correction of 30 degrees. The linear velocity model considered here, as previously stated, is $v(z)$=1.5+0.6z km/s. tariq1-Op2reslin30on [NR]

Figure 16 includes residual AMO operators for corrections in offset, as well as azimuth, for the linear velocity model. However, the residual operator corresponding to a correction in azimuth only (middle), is smaller in size than the operators that include an offset correction as well (right), or has only an offset correction (left). The crossline component of the residual AMO operator that includes offset correction is

important, because in homogeneous media the offset-correction operator does not include a crossline component. In fact, the size of the crossline component of the residual AMO operator corresponding to a purely offset correction should be about the same as the crossline component of the AMO operator for a similar correction, shown in Figure 6 (upper-left). In other words, the convolution of the residual DMO operator for a homogeneous medium, which is a 2-D operator, with the residual AMO operator in Figure 16 (left) should give us the AMO operator, shown in Figure 6 (upper-left). As expected, all residual AMO operators for the linear velocity case are smooth. Not so, for the low-velocity-layer case, where the perturbation of the model from a

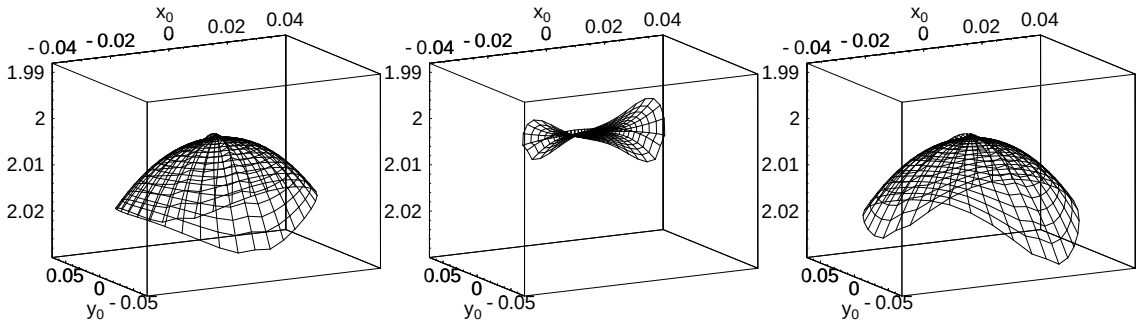

Figure 16: Residual AMO operators corresponding to the difference between AMO operators in a homogeneous medium and AMO operators in the linear velocity medium. Both media have the same rms velocity at the NMO corrected time of 2 s. Left: corresponds to the AMO operator with a correction in offset from 2 to 1.5 km. Middle: corresponds to the AMO operator with a correction in azimuth only of 30 degrees. Right: corresponds to the AMO operator with a correction in offset and azimuth. tariq1-Op3vzreslin [NR]

homogeneous background caused, among other things, huge triplications. However, the residual operator, even for this case is generally small. Therefore, the correction needed to adjust for the low-velocity layer model, when a homogeneous AMO is applied, is generally small. In fact, it is as small as the linear velocity case model. Again, the residual operator corresponding to a correction in azimuth is the smallest.

For the case of the complicated high-velocity layer the observations are different. Even for the purely azimuth-correction operator, the residual operator, shown in Figure 18, is both complicated and large. In fact, the size of the residual AMO operator is almost the same as the size of the full AMO operator. The unequal distribution of ray parameters, as shown by the top view of Figure 18, suggests that steep angle dips are affected the most by applying a constant-velocity AMO operator. While reflections from small dip angles are generally helped the constant-velocity AMO operator. Figure 19 shows the full range of residual AMO operators corresponding to correction in azimuth and offset. All operators have complicated shapes, however, now the size of the residual AMO operator corresponding to offset correction only is smaller than those that include azimuth correction. This reversal

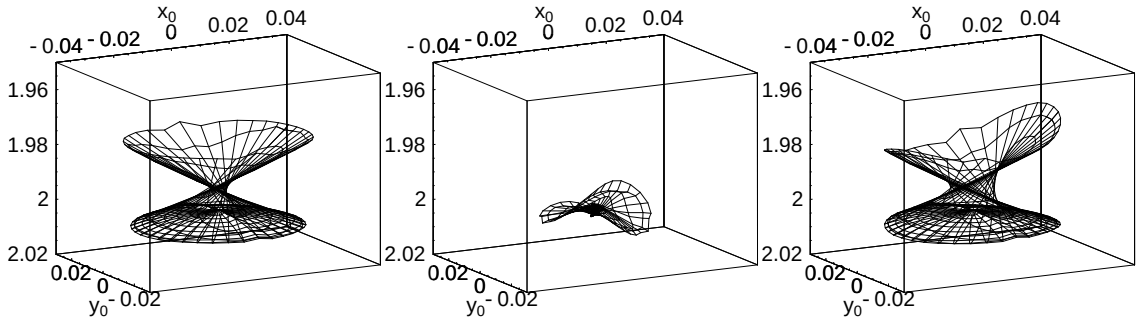

Figure 17: Residual AMO operators for the difference between AMO operators in a homogeneous medium and the low-velocity-layer medium. Both media have the same rms velocity at the NMO corrected time of 2 s. Left: corresponds to the AMO operator with a correction in offset from 2 to 1.5 km. Middle: corresponds to the AMO operator with a correction in azimuth of 30 degrees. Right: corresponds to the AMO operator with a correction in offset and azimuth. tariq1-Op3vzreslow [NR]

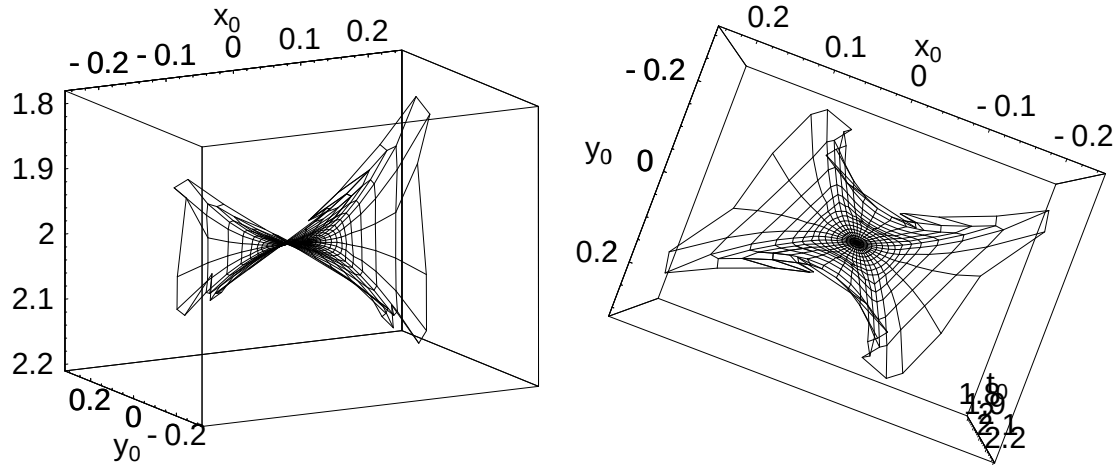

Figure 18: A side (left) and a top (right) view of a residual AMO operator responsible for the correction from the high-velocity-layer model in Figure 5 (left) to a homogeneous medium for a pure azimuth correction of 30 degrees. tariq1-Op2vzreshigh [NR]

in size implies that such a velocity model impacts the azimuth correction more than the offset correction. This is a general statement, however a more accurate conclusion should include constant ray parameter comparisons, not shown here.

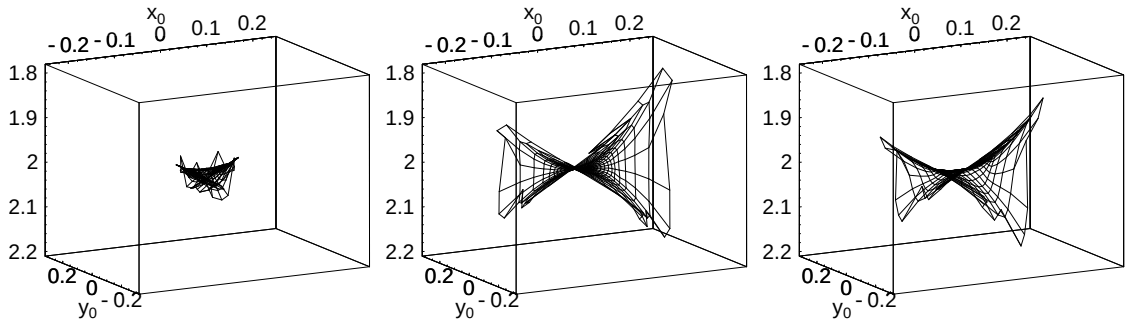

Figure 19: Residual AMO operators for the difference between AMO operators in a homogeneous medium and the high-velocity-layer medium. Both media have the same rms velocity at the NMO corrected time of 2 s. Left: corresponds to the AMO operator with a correction in offset from 2 to 1.5 km. Middle: corresponds to the AMO operator with a correction in azimuth of 30 degrees. Right: corresponds to the AMO operator with a correction in offset and azimuth. tariq1-Op3vzreshigh [NR]

The residual AMO operator in Figure 19 (left), that is responsible for offset correction, seems extremely complicated. The inline and crossline component of that operator, shown in Figure 20, displays the large number of triplications associated with the operator.

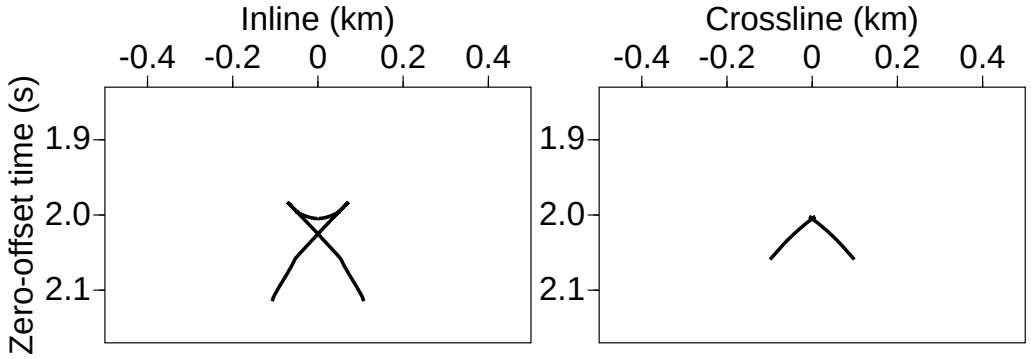

Figure 20: The inline and crossline components of the residual AMO operator shown in Figure 19 (left), but with a wider aperture. tariq1-incrossvzhighres [NR]

COST ISSUES

The computation cost of applying the 3-D AMO or DMO operators is an order magnitude higher than that for 2-D ones. However, the computational cost is also directly dependent on the size of the operator. Therefore, for a simple Kirchhoff-type implementation (Deregowski, 1995), the cost of the 3-D AMO operator is proportional to the product of the inline and crossline grid points needed to represent the operator. Luckly, AMO operators are generally small in size, and as a result, the number of grid points in which the operator covers are relatively few. In the application of 3-D operators, the reduction in the size of the operator is far more important than in 2-D media.

CONCLUSIONS

For smooth vertical inhomogeneities, the AMO operator has a shape and size similar to its homogeneous medium counterpart; a general skewed saddle shape. This is especially the case when the AMO operator includes only azimuth corrections. In fact, such an operator is also free of triplications, which will ease its use in practice. AMO operators that include offset correction, often show triplications. In general, AMO operators that correct only the azimuth are much simpler than those that also correct the offset. Therefore, using such operators in Kirchhoff-type implementation, should be straightforward.

The residual operators, derived by cascading a forward homogeneous-medium AMO and an inverse $v(z)$ AMO, confirm the small difference in AMO between the two media. In fact, for the linear and low-velocity zone examples the vertical size of the operator is less than 10 ms. This is not the case for the complicated high-velocity layer model, where the residual AMO operator has almost the size of the full AMO operator.

The computational efficiency of a Kirchhoff-type AMO implementation depends largely on the size of the AMO operator. We have shown that for smooth $v(z)$ media, as for homogeneous media, the AMO operator is generally small.

REFERENCES

Artley, C., Blondel, P., Popovici, A. M., and Schwab, M., 1993, Equations for three dimensional dip moveout in depth-variable velocity media: SEP–**77**, 43–48.

Biondi, B., Fomel, S., and Chemingui, N., 1998, Azimuth moveout for 3-d prestack imaging: Geophysics, **63**, 574–588.

Biondi, B., 1998, Azimuth moveout vs. dip moveout in inhomogeneous media: SEP–**97**, 83–94.

Deregowski, S. M., 1995, An integral implementation of dip moveout, *in* Hale, D., Ed., DMO processing: Soc. Expl. Geophys., 177–188.

Hanson, D. W., and Witney, S. A., 1995, 3-D prestack depth migration – velocity model building and case history: 1995 Spring Symposium of the Geophys. Soc. of Tulsa, Soc. Expl. Geophys., Seismic Depth Estimation, 27–52.